How Well Do We Know the Neutron-Matter Equation of State at the Densities Inside Neutron Stars? A Bayesian Approach with Correlated Uncertainties

C. Drischler,[1,2,*] R. J. Furnstahl,[3,†] J. A. Melendez,[3,‡] and D. R. Phillips[4,§]
[1]Department of Physics, University of California, Berkeley, California 94720, USA
[2]Nuclear Science Division, Lawrence Berkeley National Laboratory, Berkeley, California 94720, USA
[3]Department of Physics, The Ohio State University, Columbus, Ohio 43210, USA
[4]Department of Physics and Astronomy and Institute of Nuclear and Particle Physics, Ohio University, Athens, Ohio 45701, USA

(Received 25 April 2020; revised 28 July 2020; accepted 25 September 2020; published 11 November 2020)

We introduce a new framework for quantifying correlated uncertainties of the infinite-matter equation of state derived from chiral effective field theory (χEFT). Bayesian machine learning via Gaussian processes with physics-based hyperparameters allows us to efficiently quantify and propagate theoretical uncertainties of the equation of state, such as χEFT truncation errors, to derived quantities. We apply this framework to state-of-the-art many-body perturbation theory calculations with nucleon-nucleon and three-nucleon interactions up to fourth order in the χEFT expansion. This produces the first statistically robust uncertainty estimates for key quantities of neutron stars. We give results up to twice nuclear saturation density for the energy per particle, pressure, and speed of sound of neutron matter, as well as for the nuclear symmetry energy and its derivative. At nuclear saturation density, the predicted symmetry energy and its slope are consistent with experimental constraints.

DOI: 10.1103/PhysRevLett.125.202702

Introduction.—How well do we know the neutron-matter equation of state (EOS) at the densities inside neutron stars? This is a key question for nuclear (astro)physics in the era of multimessenger astronomy. To answer this question from nuclear theory requires a systematic understanding of strongly interacting, neutron-rich matter at densities several times the typical density in heavy nuclei, i.e., well beyond the nuclear saturation density $n_0 \approx 0.16$ fm^{-3} ($\rho_0 \approx 2.7 \times 10^{14}$ g cm^{-3}). The dominant microscopic approach to describing nuclear forces at low energies is chiral effective field theory (χEFT) with nucleon and pion degrees of freedom [1–4]. It has made great progress in predicting the EOS of infinite (nuclear) matter and the structure of neutron stars at densities $\lesssim n_0$ [5–19] (see also Refs. [20–22] for recent reviews). But the truncation errors inherent in χEFT grow dramatically with density [18,23–26]. Existing predictions only provide rough estimates for them and do not account for correlations within or between observables.

In this Letter, we use a novel Bayesian approach to quantify the truncation errors in χEFT predictions for pure neutron matter (PNM) at zero temperature [27,28]. The EOS is obtained from state-of-the-art many-body perturbation theory (MBPT) calculations with nucleon-nucleon (NN) and three-nucleon (3N) interactions up to fourth order in the χEFT expansion (i.e., next-to-next-to-next-to-leading order, N^{3}LO) [17]. Our algorithm accounts for correlations in EOS truncation errors—both across densities and between observables—enabling us to obtain reliable uncertainties for physical properties derived from the EOS, e.g., the pressure and the speed of sound. This significant advance in uncertainty quantification (UQ) is timely given the need for statistically robust comparisons [29] between nuclear theory and recent observational constraints [30–37].

χEFT is a systematic expansion in powers of a typical momentum scale, p, over the EFT breakdown scale, Λ_b. For infinite matter, p is of order the nucleon Fermi momentum k_F. Provided $k_F < \Lambda_b$, χEFT calculations of strongly interacting matter can be improved to any desired accuracy. In practice, there is always a discrepancy between the χEFT result and reality because observables are calculated at a finite order in the expansion, leaving a residual error that must be quantified [38–40].

Melendez *et al.* [27] developed a Bayesian model for EFT truncation errors that accounts for uncertainties that vary smoothly with independent variable(s)—in this case k_F or the nucleon density n. A machine-learning algorithm is trained on the computed orders in the χEFT expansion, from which it learns the magnitude of the truncation error and its correlations in density. In a companion publication [28], we apply this new approach to infinite matter. This provides the first estimates of in-medium EFT breakdown scales and nuclear saturation properties with correlated EFT truncation errors. We also uncover a strong correlation between PNM and symmetric nuclear matter (SNM) for the χEFT Hamiltonians of interest. This is crucial to the UQ of the nuclear symmetry energy we present here.

This Letter focuses on PNM and, together with its companion paper [28], sets a new standard for UQ in infinite-matter calculations based on χEFT. (See Section IV. 2 in Ref. [41] for an overview of other recent applications of machine learning and Bayesian methods in low-energy nuclear theory.) We first review definitions relevant to our study: the energy per particle, pressure, and speed of sound, along with the symmetry energy and its slope. Next we explain how machine-learning algorithms can estimate statistically robust, correlated uncertainties for these observables. We then provide our results and show that, for the symmetry energy and its slope at saturation density, they are in accord with experimental and theoretical constraints. The annotated Jupyter notebooks we used for the UQ of infinite-matter observables and their derivatives are publicly available [42].

Equation of state.—We consider the standard (quadratic) expansion of the infinite-matter EOS as a function of the total density $n = n_n + n_p$ and isospin asymmetry $\beta = (n_n - n_p)/n$,

$$\frac{E}{A}(n,\beta) \approx \frac{E}{A}(n,\beta=0) + \beta^2 S_2(n), \tag{1}$$

about SNM ($\beta = 0$); with the neutron (proton) density given by n_n (n_p). Microscopic asymmetric matter calculations based on chiral NN and 3N interactions at $n \lesssim n_0$ have shown that this expansion works reasonably well [8,43] (cf. Refs. [44,45]). The density-dependent symmetry energy $S_2(n)$ is then given by the difference between the energy per particle in PNM (E/N) and SNM (E/A),

$$S_2(n) \approx \frac{E}{N}(n) - \frac{E}{A}(n) \equiv S_v + \frac{L}{3}\left(\frac{n-n_0}{n_0}\right) + \cdots. \tag{2}$$

We focus our analysis on four key quantities for PNM and neutron stars. The first two are $S_2(n)$ and its (rescaled) density-dependent derivative $L(n) \equiv 3n(d/dn)S_2(n)$. When evaluated at n_0 these become, respectively, $S_v \equiv S_2(n_0)$ and $L \equiv L(n_0)$. The other two quantities are the pressure

$$P(n) = n^2 \frac{d}{dn}\frac{E}{N}(n), \tag{3}$$

and the speed of sound squared,

$$c_s^2(n) = \frac{\partial P(n)}{\partial \varepsilon(n)} = \frac{\partial P(n)}{\partial n}\left[\left(1 + n\frac{\partial}{\partial n}\right)\frac{E}{N}(n) + m_n\right]^{-1}. \tag{4}$$

Note that the energy density $\varepsilon(n) = n[(E/N)(n) + m_n]$ includes the neutron rest mass energy m_n (with $c^2 = 1$).

The central many-body inputs of our analysis are $(E/N)(n)$ and $(E/A)(n)$ as obtained in MBPT. We extend the neutron-matter calculations in Ref. [17] to $2n_0$ and use the results reported in Refs. [17,23] for SNM. The high-order MBPT calculations are driven by the novel Monte Carlo framework introduced by Drischler *et al.* [17]. It uses automatic code generation to efficiently evaluate arbitrary interaction and many-body diagrams, facilitating calculations with controlled many-body uncertainties (for details see Ref. [17]).

Reference [17] also constructed a family of order-by-order chiral NN and 3N potentials up to N^{3}LO. The NN potentials by Entem, Machleidt, and Nosyk [46] with momentum cutoffs $\Lambda = 450$ and 500 MeV were combined with 3N interactions at the same order and cutoff. The two 3N low-energy couplings c_D and c_E were fit to the triton and the empirical saturation point of SNM. These intermediate- and short-range 3N interactions, respectively, do not contribute to $(E/N)(n)$ with nonlocal regulators [47]. There is consequently only one neutron-matter EOS determined for each cutoff and χEFT order [17]. Our results for a given cutoff do not differ significantly for the different 3N fits. We restrict the discussion here to the $\Lambda = 500$ MeV potentials of Ref. [17] with $c_D = -1.75$ (-3.00) and $c_E = -0.64$ (-2.22) at N^{2}LO (N^{3}LO) and refer to the Supplemental Material [48] for results with the other cutoff. More details on these Hamiltonians can be found in Refs. [17,28].

Uncertainty quantification.—Our truncation-error model relies on Gaussian processes (GPs), a machine-learning algorithm, to uncover the size and smoothness properties of the EFT uncertainty [49]. We train physically motivated GPs from our UQ framework to the order-by-order predictions of $(E/N)(n)$ and $(E/A)(n)$, leading to smooth regression curves. Training refers here to both estimating the GP hyperparameters (e.g., Λ_b and the GP correlation length) and finding the regression curve. Note that this requires choices for the functional form of the EFT expansion parameter and a reference scale for each observable, as discussed in Refs. [27,28]. The resulting curves also include an interpolation uncertainty that accounts for many-body uncertainties in the training data. Reference [17] showed that the residual many-body uncertainty is much smaller than the χEFT truncation error for the interactions considered here. Nevertheless, to be conservative, we set this additional interpolation uncertainty to 0.1% of the total energy per particle (but ≥ 20 keV). The results are insensitive to that choice.

An important byproduct of finding the optimal regression curves is a Gaussian posterior for the truncation error that includes correlations in density. Combining the respective regression curve with the interpolation and EFT truncation uncertainties produces a GP for each EOS from the to-all-orders EFT. Furthermore, GPs are closed under differentiation. It is then straightforward to compute a joint distribution that includes correlations between the EOS and its derivatives [50–53].

But assessing the uncertainty in $S_2(n)$ requires an additional step. We have found that $(E/N)(n)$ and

$(E/A)(n)$ converge in a similar fashion [28]; given an EFT correction of $(E/N)(n)$, it is likely that the correction to $(E/A)(n)$ will have the same sign. This additional correlation *between* observables implies that the truncation error in $S_2(n)$ is less than the in-quadrature sum of errors from PNM and SNM. Our truncation framework naturally extends to this case via *multitask* machine learning (for details see Ref. [28]; also [54–57]). The correlation found with multitask GPs precisely matches the empirical correlation.

Our novel framework thus permits the efficient evaluation of arbitrary derivatives and the full propagation of uncertainties within and between observables. Each type of correlation is essential for full UQ in infinite matter: without correlations in density, derivatives of the EOS would have grossly exaggerated uncertainties; without correlations between observables and their derivatives, UQ for $c_s^2(n)$ would not be reliable; without correlations between PNM and SNM, the uncertainty on $S_2(n)$ and $L(n)$ would be overestimated. More details can be found in Refs. [27,28].

Results.—Figure 1 shows our order-by-order χEFT predictions, up to N^{3}LO, for $(E/N)(n)$, $P(n)$, and $c_s^2(n)$ in PNM, as well as $S_2(n)$, $L(n)$, and $(E/A)(n)$. We find an EFT breakdown scale Λ_b consistent with 600 MeV and optimized truncation-error correlation lengths $\ell = 0.97$ fm^{-1} (0.48 fm^{-1}) for PNM (SNM). The correlation between the truncation errors of $(E/N)(n)$ and $(E/A)(n)$ is $\rho = 0.94$. These hyperparameters are only tuned to the derivative-free quantities $(E/N)(n)$ and $(E/A)(n)$; derivatives and their uncertainties are thus *pure predictions* of our framework, as are $S_2(n)$ and $L(n)$. The bands in Fig. 1 account for both the EFT truncation error and the overall interpolation uncertainty. Our Bayesian 1σ uncertainties for derivative-free quantities are broadly similar [39] to those obtained using the "standard EFT" error prescription [58–61], e.g., as it was applied to UQ of the EOS in Ref. [17]. But only our correlated approach can propagate these reliably to $P(n)$, $S_2(n)$, $L(n)$, and $c_s^2(n)$.

We observe an order-by-order EFT convergence pattern for the observables at low densities, $n \lesssim 0.1$ fm^{-3}. However, at N^{2}LO and beyond, 3N interactions enter the χEFT expansion with repulsive contributions, especially at densities $n \gg n_0$. Their N^{2}LO and N^{3}LO EFT corrections then have a markedly different density dependence, as indicated by our model-checking diagnostics [27] for each energy per particle [28]. This produces bands that do not appear to encapsulate higher-order predictions. Nevertheless, we stress caution when critiquing the consistency of the uncertainty bands; because of the strong correlations, statistical fluctuations can occur over large ranges in density. Our credible interval diagnostics show that the bands are consistent up to these fluctuations [28].

The distributions of all observables follow a multivariate Gaussian except for $c_s^2(n)$, which requires sampling.

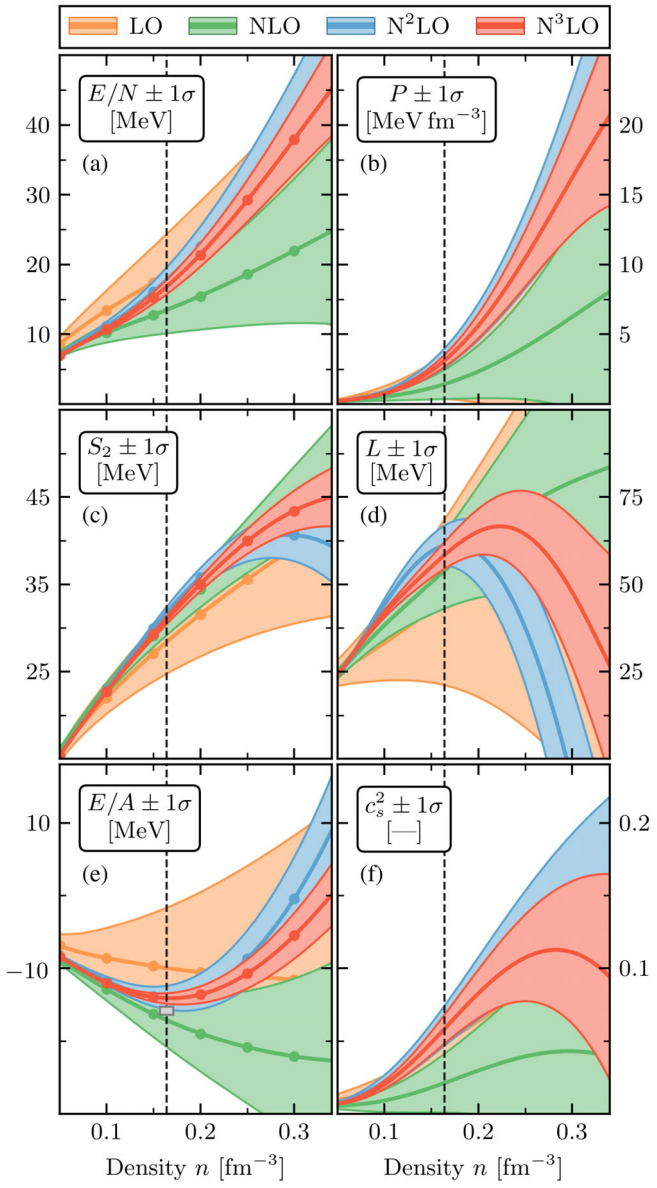

FIG. 1. Order-by-order predictions with 68% bands for (a) the energy per particle $(E/N)(n)$ and (b) the pressure $P(n)$ of PNM; (c) the symmetry energy $S_2(n)$ and (d) its (rescaled) density dependence $L(n)$; (e) the energy per particle $(E/A)(n)$ of SNM; and (f) the speed of sound $c_s^2(n)$ of PNM, each as a function of density. Dots denote every fifth interpolation point, where $n = 0.05, 0.06, \ldots, 0.34$ fm^{-3}. The gray box in (e) depicts the empirical saturation point, $n_0 = 0.164 \pm 0.007$ fm^{-3} with $(E/A)(n_0) = -15.86 \pm 0.57$ MeV, obtained from a set of energy density functionals [17,43]. The vertical lines are located at $n = 0.164$ fm^{-3}. See the main text for details.

The strong correlation between $(E/N)(n)$ and $(E/A)(n)$ produces narrow constraints at n_0: $S_v = 31.7 \pm 1.1$ MeV and $L = 59.8 \pm 4.1$ MeV at the 1σ level. These agree remarkably well with central values from the analyses compiled in Ref. [62]. Our results for $c_s^2(n)$ are below the asymptotic high-density limit predicted by perturbative

quantum chromodynamics, $c_s^2(n \gg 50n_0) = \frac{1}{3}$ [63]. The uncertainties, however, are sizeable at the maximum density: $c_s^2(2n_0) \simeq 0.14 \pm 0.08$ (N^{2}LO) and $c_s^2(2n_0) \simeq 0.10 \pm 0.07$ (N^{3}LO). Precise measurements of neutron stars with mass $\gtrsim 2\ \mathrm{M}_\odot$ [64–67] indicate that the limit has to be exceeded in some density regime beyond n_0 [68]. Our 2σ uncertainty bands are consistent with this happening slightly above $2n_0$, especially since the downward turn of c_s^2 ($n \gtrsim 0.28\ \mathrm{fm}^{-3}$) is likely an edge effect that will disappear if we train on data at even higher densities.

Comparison to experiment.—Figure 2 depicts constraints in the S_v–L plane. The allowed region we derive from χEFT calculations of infinite matter is shown as the yellow ellipses (dark: 1σ, light: 2σ) and denoted "GP-B" (Gaussian process–BUQEYE collaboration). Also shown are several experimental and theoretical constraints compiled by Lattimer *et al.* [69–71]. The experimental constraints include measurements of isoscalar giant dipole resonances, dipole polarizabilities, and neutron-skin thicknesses (see the caption for details). The white area depicts the intersection of all these (excluding that from isobaric analog states and isovector skins, which barely overlaps). This region is in excellent agreement with our prediction.

Our yellow ellipses in Fig. 2 represent the posterior $\mathrm{pr}(S_v, L \,|\, \mathcal{D})$, where the training data $\mathcal{D}$ are the order-by-order predictions of $(E/N)(n)$ and $(E/A)(n)$ up to $2n_0$. The distribution is accurately approximated by a two-dimensional Gaussian with mean and covariance

$$\begin{bmatrix} \mu_{S_v} \\ \mu_L \end{bmatrix} = \begin{bmatrix} 31.7 \\ 59.8 \end{bmatrix} \quad \text{and} \quad \Sigma = \begin{bmatrix} 1.11^2 & 3.27 \\ 3.27 & 4.12^2 \end{bmatrix}. \quad (5)$$

We consider all likely values of n_0 via $\mathrm{pr}(S_v, L \,|\, \mathcal{D}) = \int \mathrm{pr}(S_2, L \,|\, n_0, \mathcal{D}) \mathrm{pr}(n_0 \,|\, \mathcal{D}) dn_0$. Here, $\mathrm{pr}(S_2, L \,|\, n_0, \mathcal{D})$ describes the correlated to-all-orders predictions at a particular density n_0, and $\mathrm{pr}(n_0 \,|\, \mathcal{D}) \approx 0.17 \pm 0.01\ \mathrm{fm}^{-3}$ is the Gaussian posterior for the saturation density, including truncation errors, determined in Ref. [28]. If the canonical empirical saturation density, $n_0 = 0.164\ \mathrm{fm}^{-3}$, is used instead the posterior mean shifts slightly downwards: $S_v \to S_v - 0.8$ MeV and $L \to L - 1.4$ MeV. This shift is well within the uncertainties computed using our internally consistent n_0. In contrast to experiments, which extract S_v–L from measurements over a range of densities, our theoretical approach predicts directly at saturation density, thereby removing artifacts induced by extrapolation.

Our 2σ ellipse falls completely within constraints derived from the conjecture that the unitary gas is a lower limit on the EOS [69] (solid black line). The same work also made additional simplifying assumptions to derive an analytic bound—only our 1σ ellipse is fully within that region (dashed black line). Figure 2 also shows the allowed regions obtained from microscopic neutron-matter calculations by Hebeler *et al.* [79] (based on χEFT NN and 3N interactions fit to few-body data only) and Gandolfi *et al.* [80] (where 3N interactions were adjusted to a range of S_v). The predicted ranges in S_v agree with ours, but we find that L is ≈10 MeV larger, corresponding to a stronger density-dependence of $S_2(n_0)$. References [79,80] quote relatively narrow ranges for S_v–L, but those come from surveying available parameters in the Hamiltonians and so, unlike our quoted intervals, do not have a statistical interpretation.

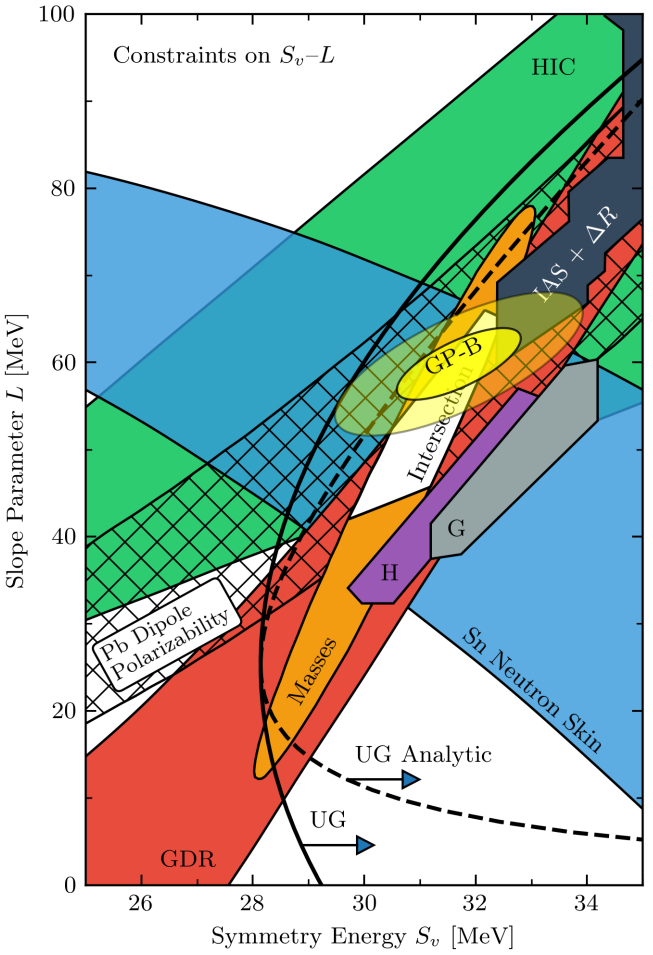

FIG. 2. Constraints on the S_v–L correlation. Our results ("GP–B") are given at the 68% (dark-yellow ellipse) and 95% level (light-yellow ellipse). Experimental constraints are derived from heavy-ion collisions (HIC) [72], neutron-skin thicknesses of Sn isotopes [73], giant dipole resonances (GDR) [74], the dipole polarizability of ^{208}Pb [75,76], and nuclear masses [77]. The intersection is depicted by the white area, which only barely overlaps with constraints from isobaric analog states and isovector skins (IAS + ΔR) [78]. In addition, theoretical constraints derived from microscopic neutron-matter calculations by Hebeler *et al.* (H) [79] and Gandolfi *et al.* (G) [80] as well as from the unitary gas (UG) limit by Tews *et al.* [69]. The figure has been adapted from Refs. [70,71]. A Jupyter notebook that generates it is provided in Ref. [42].

Summary and outlook.—We presented a novel framework for EFT truncation errors that includes correlations

within and between observables. It enables the efficient evaluation of derived quantities. We then constrained multiple key observables for neutron-star physics based on cutting-edge MBPT calculations with χEFT NN and 3N interactions up to N^{3}LO. Correlations in the EFT truncation error—both across densities and between different observables—must be accounted for in order to obtain full credible intervals. In several cases (e.g., S_v) the result is a much smaller uncertainty than one might naïvely expect. Our narrow predictions for S_v–L are in excellent agreement with the joint experimental constraint.

A rigorous comparison between empirical constraints on the EOS and our knowledge of the underlying microscopic dynamics of strongly interacting nuclear matter is particularly important in the era of multimessenger astronomy because new constraints on the neutron-star EOS are anticipated from NASA's NICER [33–36] and from the LIGO-Virgo collaboration [30–32]. Our EOS results are in good agreement with recent observations, especially those with input from NICER (cf. theory-agnostic joint observational posteriors in Figure 1 of Ref. [37]). Nuclear physics experiments (e.g., those in Refs. [81–84]) will also contribute important information to this overall picture.

Our Bayesian framework can be straightforwardly adapted and used in future studies that will more firmly establish this comparison. A full Bayesian analysis can be performed via Markov Chain Monte Carlo sampling over GP hyperparameters and the low-energy couplings in the nuclear interactions [40,85,86]. This requires the development of improved chiral NN and 3N forces up to N^{3}LO [87–89]. Extensions to arbitrary isospin asymmetry and finite temperature are also an important avenue for future study. Work in all these directions will be facilitated by the public availability of the tools presented here as Jupyter notebooks [42].

We thank S. Reddy for fruitful discussions. We are also grateful to the organizers of "Bayesian Inference in Subatomic Physics—A Marcus Wallenberg Symposium" at Chalmers University of Technology, Gothenburg for creating a stimulating environment to learn and discuss the use of statistical methods in nuclear physics. C. D. acknowledges support by the Alexander von Humboldt Foundation through a Feodor-Lynen Fellowship and the U.S. Department of Energy, the Office of Science, the Office of Nuclear Physics, and SciDAC under Awards No. DE-SC00046548 and No. DE-AC02-05CH11231. The work of R. J. F. and J. A. M. was supported in part by the National Science Foundation under Grants No. PHY–1614460 and No. PHY–1913069, and the NUCLEI SciDAC Collaboration under U.S. Department of Energy MSU subcontract RC107839-OSU. The work of D. R. P. was supported by the U.S. Department of Energy under Award No. DE-FG02-93ER-40756 and by the National Science Foundation under PHY-1630782, N3AS FRHTP. C. D. thanks the Physics Departments of The Ohio State University and Ohio University for their warm hospitality during extended stays in the BUQEYE state.

*Corresponding author.
cdrischler@berkeley.edu
†Corresponding author.
furnstahl.1@osu.edu
‡Corresponding author.
melendez.27@osu.edu
§Corresponding author.
phillid1@ohio.edu

[1] E. Epelbaum, H.-W. Hammer, and U.-G. Meißner, Rev. Mod. Phys. **81**, 1773 (2009).
[2] R. Machleidt and D. R. Entem, Phys. Rep. **503**, 1 (2011).
[3] H. W. Hammer, S. König, and U. van Kolck, Rev. Mod. Phys. **92**, 025004 (2020).
[4] I. Tews, Z. Davoudi, A. Ekström, J. D. Holt, and J. E. Lynn, J. Phys. G **47**, 103001 (2020).
[5] I. Tews, T. Krüger, K. Hebeler, and A. Schwenk, Phys. Rev. Lett. **110**, 032504 (2013).
[6] K. Hebeler, J. M. Lattimer, C. J. Pethick, and A. Schwenk, Astrophys. J. **773**, 11 (2013).
[7] G. Baardsen, A. Ekström, G. Hagen, and M. Hjorth-Jensen, Phys. Rev. C **88**, 054312 (2013).
[8] C. Drischler, V. Somà, and A. Schwenk, Phys. Rev. C **89**, 025806 (2014).
[9] G. Hagen, T. Papenbrock, A. Ekström, K. Wendt, G. Baardsen, S. Gandolfi, M. Hjorth-Jensen, and C. Horowitz, Phys. Rev. C **89**, 014319 (2014).
[10] A. Carbone, A. Polls, and A. Rios, Phys. Rev. C **88**, 044302 (2013).
[11] L. Coraggio, J. W. Holt, N. Itaco, R. Machleidt, L. E. Marcucci, and F. Sammarruca, Phys. Rev. C **89**, 044321 (2014).
[12] C. Wellenhofer, J. W. Holt, N. Kaiser, and W. Weise, Phys. Rev. C **89**, 064009 (2014).
[13] A. Roggero, A. Mukherjee, and F. Pederiva, Phys. Rev. Lett. **112**, 221103 (2014).
[14] J. W. Holt and N. Kaiser, Phys. Rev. C **95**, 034326 (2017).
[15] C. Drischler, A. Carbone, K. Hebeler, and A. Schwenk, Phys. Rev. C **94**, 054307 (2016).
[16] A. Ekström, G. Hagen, T. D. Morris, T. Papenbrock, and P. D. Schwartz, Phys. Rev. C **97**, 024332 (2018).
[17] C. Drischler, K. Hebeler, and A. Schwenk, Phys. Rev. Lett. **122**, 042501 (2019).
[18] D. Lonardoni, I. Tews, S. Gandolfi, and J. Carlson, Phys. Rev. Research **2**, 022033 (2020).
[19] M. Piarulli, I. Bombaci, D. Logoteta, A. Lovato, and R. B Wiringa, Phys. Rev. C **101**, 045801 (2020).
[20] K. Hebeler, J. D. Holt, J. Menéndez, and A. Schwenk, Annu. Rev. Nucl. Part. Sci. **65**, 457 (2015).
[21] C. Drischler, W. Haxton, K. McElvain, E. Mereghetti, A. Nicholson, P. Vranas, and A. Walker-Loud, arXiv:1910.07961.
[22] F. Sammarruca and R. Millerson, Front. Phys. **7**, 213 (2019).
[23] M. Leonhardt, M. Pospiech, B. Schallmo, J. Braun, C. Drischler, K. Hebeler, and A. Schwenk, Phys. Rev. Lett. **125**, 142502 (2020).

[24] I. Tews, J. Margueron, and S. Reddy, Eur. Phys. J. A **55**, 97 (2019).
[25] I. Tews, J. Margueron, and S. Reddy, Phys. Rev. C **98**, 045804 (2018).
[26] I. Tews, J. Carlson, S. Gandolfi, and S. Reddy, Astrophys. J. **860**, 149 (2018).
[27] J. A. Melendez, R. J. Furnstahl, D. R. Phillips, M. T. Pratola, and S. Wesolowski, Phys. Rev. C **100**, 044001 (2019).
[28] C. Drischler, J. A. Melendez, R. J. Furnstahl, and D. R. Phillips, companion paper, Phys. Rev. C **102**, 054315 (2020).
[29] The Editors, Phys. Rev. A **83**, 040001 (2011).
[30] B. P. Abbott *et al.* (LIGO Scientific, Virgo, Fermi GBM, INTEGRAL, IceCube, AstroSat Cadmium Zinc Telluride Imager Team, IPN, Insight-Hxmt, ANTARES, Swift, AGILE Team, 1M2H Team, Dark Energy Camera GW-EM, DES, DLT40, GRAWITA, Fermi-LAT, ATCA, ASKAP, Las Cumbres Observatory Group, OzGrav, DWF (Deeper Wider Faster Program), AST3, CAASTRO, VINROUGE, MASTER, J-GEM, GROWTH, JAGWAR, CaltechNRAO, TTU-NRAO, NuSTAR, Pan-STARRS, MAXI Team, TZAC Consortium, KU, Nordic Optical Telescope, ePESSTO, GROND, Texas Tech University, SALT Group, TOROS, BOOTES, MWA, CALET, IKI-GW Follow-up, H.E.S.S., LOFAR, LWA, HAWC, Pierre Auger, ALMA, Euro VLBI Team, Pi of Sky, Chandra Team at McGill University, DFN, ATLAS Telescopes, High Time Resolution Universe Survey, RIMAS, RATIR, and SKA South Africa/MeerKAT Collaborations), Astrophys. J. **848**, L12 (2017).
[31] B. P. Abbott *et al.* (LIGO Scientific and Virgo Collaborations), Phys. Rev. Lett. **121**, 161101 (2018).
[32] B. P. Abbott *et al.* (LIGO Scientific and Virgo Collaborations), Phys. Rev. X **9**, 011001 (2019).
[33] S. Bogdanov, F. K. Lamb, S. Mahmoodifar, M. C. Miller, S. M. Morsink, T. E. Riley, T. E. Strohmayer, A. K. Tung, A. L. Watts, A. J. Dittmann, D. Chakrabarty, S. Guillot, Z. Arzoumanian, and K. C. Gendreau, Astrophys. J. **887**, L26 (2019).
[34] T. E. Riley, A. L. Watts, S. Bogdanov, P. S. Ray, R. M. Ludlam, S. Guillot, Z. Arzoumanian, C. L. Baker, A. V. Bilous, D. Chakrabarty, K. C. Gendreau, A. K. Harding, W. C. G. Ho, J. M. Lattimer, S. M. Morsink, and T. E. Strohmayer, Astrophys. J. **887**, L21 (2019).
[35] M. C. Miller *et al.*, Astrophys. J. **887**, L24 (2019).
[36] G. Raaijmakers, T. E. Riley, A. L. Watts, S. K. Greif, S. M. Morsink, K. Hebeler, A. Schwenk, T. Hinderer, S. Nissanke, S. Guillot, Z. Arzoumanian, S. Bogdanov, D. Chakrabarty, K. C. Gendreau, W. C. G. Ho, J. M. Lattimer, R. M. Ludlam, and M. T. Wolff, Astrophys. J. **887**, L22 (2019).
[37] R. Essick, I. Tews, P. Landry, S. Reddy, and D. E. Holz, Phys. Rev. C **102**, 055803 (2020).
[38] R. J. Furnstahl, D. R. Phillips, and S. Wesolowski, J. Phys. G **42**, 034028 (2015).
[39] R. J. Furnstahl, N. Klco, D. R. Phillips, and S. Wesolowski, Phys. Rev. C **92**, 024005 (2015).
[40] S. Wesolowski, N. Klco, R. J. Furnstahl, D. R. Phillips, and A. Thapaliya, J. Phys. G **43**, 074001 (2016).
[41] P. Bedaque, A. Boehnlein, M. Cromaz, M. Diefenthaler, L. Elouadrhiri, T. Horn, M. Kuchera, D. Lawrence, D. Lee, S. Lidia, R. McKeown, W. Melnitchouk, W. Nazarewicz, K. Orginos, Y. Roblin, M. Scott Smith, M. Schram, and X.-N. Wang, arXiv:2006.05422.
[42] BUQEYE collaboration, https://buqeye.github.io/software/.
[43] C. Drischler, K. Hebeler, and A. Schwenk, Phys. Rev. C **93**, 054314 (2016).
[44] N. Kaiser, Phys. Rev. C **91**, 065201 (2015).
[45] C. Wellenhofer, J. W. Holt, and N. Kaiser, Phys. Rev. C **93**, 055802 (2016).
[46] D. R. Entem, R. Machleidt, and Y. Nosyk, Phys. Rev. C **96**, 024004 (2017).
[47] K. Hebeler and A. Schwenk, Phys. Rev. C **82**, 014314 (2010).
[48] See Supplemental Material at http://link.aps.org/supplemental/10.1103/PhysRevLett.125.202702 for the corresponding results obtained using the $\Lambda = 450$ MeV potentials, a comparison of our results to the literature, and discussion of both future full Bayesian analyses and the extent of the correlations between the EOS in the limits of PNM and SNM.
[49] C. Rasmussen and C. Williams, *Gaussian Processes for Machine Learning*, Adaptive computation and machine learning series (University Press Group Limited, Cambridge, MA, 2006).
[50] C. Rasmussen, Bayesian Stat. **7**, 651 (2003).
[51] E. Solak, R. Murray-smith, W. E. Leithead, D. J. Leith, and C. E. Rasmussen, in *Advances in Neural Information Processing Systems 15*, edited by S. Becker, S. Thrun, and K. Obermayer (MIT Press, Cambridge, MA, 2003), pp. 1057–1064.
[52] D. Eriksson, K. Dong, E. Lee, D. Bindel, and A. G. Wilson, in *Advances in Neural Information Processing Systems 31*, edited by S. Bengio, H. Wallach, H. Larochelle, K. Grauman, N. Cesa-Bianchi, and R. Garnett (Curran Associates, Inc., Red Hook, 2018), pp. 6867–6877.
[53] M. Chilenski, M. Greenwald, Y. Marzouk, N. Howard, A. White, J. Rice, and J. Walk, Nucl. Fusion **55**, 023012 (2015).
[54] M. Álvarez, L. Rosasco, and N. Lawrence, *Kernels for Vector-Valued Functions: A Review*, Foundations and Trends in Machine Learning Series (Now Publishers Incorporated, Norwell, MA, 2012).
[55] A. Melkumyan and F. Ramos, in *Proceedings of the Twenty-Second International Joint Conference on Artificial Intelligence—Volume Two*, IJCAI'11 (AAAI Press, Palo Alto, CA, 2011), p. 1408–1413.
[56] R. Caruana, Mach. Learn. **28**, 41 (1997).
[57] Y. Zhang and Q. Yang, Natl. Sci. Rev. **5**, 30 (2017).
[58] D. R. Phillips, G. Rupak, and M. J. Savage, Phys. Lett. B **473**, 209 (2000).
[59] H. W. Griesshammer, J. A. McGovern, D. R. Phillips, and G. Feldman, Prog. Part. Nucl. Phys. **67**, 841 (2012).
[60] E. Epelbaum, H. Krebs, and U.-G. Meißner, Phys. Rev. Lett. **115**, 122301 (2015).
[61] E. Epelbaum, H. Krebs, and U.-G. Meißner, Eur. Phys. J. A **51**, 53 (2015).
[62] B.-A. Li, P. G. Krastev, D.-H. Wen, and N.-B. Zhang, Eur. Phys. J. A **55**, 117 (2019).
[63] E. S. Fraga, A. Kurkela, and A. Vuorinen, Astrophys. J. **781**, L25 (2014).

[64] P. Demorest, T. Pennucci, S. Ransom, M. Roberts, and J. Hessels, Nature (London) **467**, 1081 (2010).
[65] J. Antoniadis *et al.*, Science **340**, 1233232 (2013).
[66] E. Fonseca *et al.*, Astrophys. J. **832**, 167 (2016).
[67] H. T. Cromartie *et al.*, Nat. Astron. **4**, 72 (2020).
[68] P. Bedaque and A. W. Steiner, Phys. Rev. Lett. **114**, 031103 (2015).
[69] I. Tews, J. M. Lattimer, A. Ohnishi, and E. E. Kolomeitsev, Astrophys. J. **848**, 105 (2017).
[70] J. M. Lattimer and A. W. Steiner, Eur. Phys. J. A **50**, 40 (2014).
[71] J. M. Lattimer and Y. Lim, Astrophys. J. **771**, 51 (2013).
[72] M. B. Tsang, Y. Zhang, P. Danielewicz, M. Famiano, Z. Li, W. G. Lynch, and A. W. Steiner, Phys. Rev. Lett. **102**, 122701 (2009).
[73] L.-W. Chen, C. M. Ko, B.-A. Li, and J. Xu, Phys. Rev. C **82**, 024321 (2010).
[74] L. Trippa, G. Colo, and E. Vigezzi, Phys. Rev. C **77**, 061304 (R) (2008).
[75] A. Tamii, I. Poltoratska, P. von Neumann-Cosel, Y. Fujita, T. Adachi *et al.*, Phys. Rev. Lett. **107**, 062502 (2011).
[76] X. Roca-Maza, M. Brenna, G. Colò, M. Centelles, X. Viñas, B. K. Agrawal, N. Paar, D. Vretenar, and J. Piekarewicz, Phys. Rev. C **88**, 024316 (2013).
[77] T. Kortelainen, M. Lesinski, J. Moré, W. Nazarewicz, J. Sarich, N. Schunck, M. V. Stoitsov, and S. Wild, Phys. Rev. C **82**, 024313 (2010).
[78] P. Danielewicz, P. Singh, and J. Lee, Nucl. Phys. A **958**, 147 (2017).
[79] K. Hebeler, J. M. Lattimer, C. J. Pethick, and A. Schwenk, Phys. Rev. Lett. **105**, 161102 (2010).
[80] S. Gandolfi, J. Carlson, and S. Reddy, Phys. Rev. C **85**, 032801(R) (2012).
[81] C. J. Horowitz, K. S. Kumar, and R. Michaels, Eur. Phys. J. A **50**, 48 (2014).
[82] A. B. Balantekin, J. Carlson, D. J. Dean, G. M. Fuller, R. J. Furnstahl, M. Hjorth-Jensen, R. V. F. Janssens, B.-A. Li, W. Nazarewicz, F. M. Nunes, W. E. Ormand, S. Reddy, and B. M. Sherrill, Mod. Phys. Lett. A **29**, 1430010 (2014).
[83] J. Birkhan *et al.*, Phys. Rev. Lett. **118**, 252501 (2017).
[84] S. Kaufmann, J. Simonis, S. Bacca, J. Billowes, M. L. Bissell *et al.*, Phys. Rev. Lett. **124**, 132502 (2020).
[85] B. D. Carlsson, A. Ekström, C. Forssén, D. F. Strömberg, G. R. Jansen, O. Lilja, M. Lindby, B. A. Mattsson, and K. A. Wendt, Phys. Rev. X **6**, 011019 (2016).
[86] S. Wesolowski, R. J. Furnstahl, J. A. Melendez, and D. R. Phillips, J. Phys. G **46**, 045102 (2019).
[87] J. Hoppe, C. Drischler, K. Hebeler, A. Schwenk, and J. Simonis, Phys. Rev. C **100**, 024318 (2019).
[88] T. Hüther, K. Vobig, K. Hebeler, R. Machleidt, and R. Roth, Phys. Lett. B **808**, 135651 (2020).
[89] E. Epelbaum, H. Krebs, and P. Reinert, Front. Phys. **8**, 98 (2020).